

Transmission of the relativistic fermions with the pseudospin equal to one through the quasi-periodic barriers

A.M. Korol^{1,2}, N.V.Medvid², A.I.Sokolenko²*

¹ Laboratory on Quantum Theory in Linköping, ISIR, P.O. Box 8017, S-580, Linköping, Sweden

² National University for Food Technologies, Volodymyrska str., 68, Kyiv 01601, Ukraine

Corresponding author (A.M.Korol): e-mail: korolam@ukr.net

Keywords: relativistic fermions, pseudospinone, quasi-periodic barriers

PACS: 72.80.Vp., 73.21.Cd, 73.40.Gk

The focus of our work is to explore quasiparticle transmission through the quasi-periodic superlattices based on the Lieb lattice, in which the fermion pseudo-spin equals 1. We are the first to calculate and analyze the transmission spectra (quasiparticle transmission dependences on their energy) for such structures. The quasi-periodic modulation is created with the help of the external electrostatic potential in the form of the rectangular barriers located along the axis of the SL. Our observations provide that the effective Fibonacci modulation is achieved by the alternation of the potential barrier heights in the various elements of the superlattice. For the massless fermions, the quasi-periodic modulation takes place under the conditions of the oblique incidence of the particles. For the massive fermions, the quasi-periodic modulation is observed both for the oblique and the normal incidence. Besides, we define the special importance of a super Kleintunnelingband in the transmission spectra. The present study provides a thorough analysis of the transmission spectra dependence on the parameters of the problem. The conductivity of the structure considered is also analyzed. For a definite parameter set, the transmission spectra values for pseudospin-1 fermions (Lieb lattice) and those of pseudospin- $\frac{1}{2}$ (graphene) coincide. Our findings may have useful implications in the development of nanoelectronic devices based on the Lieb lattice.

1. INTRODUCTION

Recently, close attention of the researchers have been attracted to materials in which the charge carriers are characterized by a linear dispersion relation. The fabrication of graphene in 2004 has given new impetus to the investigation of these materials. Graphene reveals a number of extraordinary properties, such as the linear dispersion relation (analogy of the graphene π - electrons with the massless Dirac fermions that at low energies are described by the massless Dirac equation), the chiral nature of tunneling, the Klein paradox, high mobility of the charge carriers, the ballistic transport, the anomalous Hall effect, unusual superconductivity and spin-orbit interaction characteristics, etc.[1-5]. The phenomenon of supercollimation, as well as additional Dirac points appearance, are characteristic of the graphene-based superlattices [3, 4, 36]. It is worth mentioning that graphene is a promising material in modern electronics in terms of replacing the silicon technology.

These unique and useful graphene properties have increased scientific interest to a number of other extraordinary materials with a cone-like dispersion relation, such as the Lieb lattice, the kagome lattice, the T_3 lattice, the α - T_3 lattice and others [6-18]. Structures with

pseudospin value of the quasiparticles equal to 1 (pseudospin-1), such as the Lieb lattice, can both exist naturally and be created artificially. For example, they are an integral part of the superconducting cuprates; the corresponding optical lattices are created by means of laser beams (see, e.g. [15] and references therein). It is known that such optical lattices serve as an effective tool for exploring a number of problems in the solid-state physics ([15] and references therein). The dispersion relation in the pseudospin-1 structures consists of three parts: two of them are the Dirac cones and the third one is the “flat band” (the “dispersionless band”). Note that there is only one Dirac cone in the line-centered-square lattice (such as the Lieb one), but there are two Dirac cones in the honey-comb lattice (graphene). In the case of massless quasiparticles, the flat band crosses the Dirac point, at which the conduction and the valence bands adjoin. This band is an important element of these structures and can essentially affect their properties [6, 18, 39, 43]. The phenomenon similar to the Klein tunneling in graphene ([2]) is observed in the pseudospin-1 structures, where the potential barriers are perfectly transparent for the case of normal incidence of the quasiparticles [6-15]. This effect is a consequence of the chiral nature of the charge carriers which in turn is related to the conservation of chirality that is implicit in the Hamiltonian (the pseudospin conservation implies the absence of backscattering at normal incidence, (see e.g. [46]). The so called super Klein tunneling is even more remarkable phenomenon which manifests itself in the pseudospin-1 structures [7, 9, 15, 18]. This effect means that the potential barrier of the height U becomes perfectly transparent for energy value $E=U/2$ for all angles of incidence. The super Klein tunneling is associated with the negative index of refraction and can be used in particular for fabrication of the high-quality focusing systems [7, 18]. The minimal shot noise is also the consequence of this phenomenon [12]. The Fano-factor value is equal not to $1/3$ but to $1/4$ in the pseudospin-1 structures [12]. Note also that the electrostatic barriers are more transparent in these structures than in graphene [7] and the effect of the supercollimation can be more easily achieved in them [11]. The super Klein tunneling of massive pseudospin-1 quasiparticles depending on the location of the flat band inside the energy gap was analyzed in detail in the recent paper [39].

At the same time, it is well known that the semiconductor superlattices can play an important role in controlling electronic processes in various contemporary devices (see, e.g. [19]). Therefore, physical properties of the superlattices are being studied scrupulously around the world. Various types of the SL are considered: strictly periodic ones, disordered ones, lattices with defects, etc. Structures intermediate between the periodic and the disordered ones (in particular the quasi-periodic lattices, such as the Fibonacci and the Thue-Morse superlattices) occupy a notable place among the SL [20-35]. This is determined by their unique properties, such as the self-similarity, the Cantor nature of the energy spectrum, and others (see, e.g. [20-35]). There is a surge of interest in exploring transport properties of the quasi-periodic superlattices ([21, 25-35]). The quasi-periodical SL can have different application areas, in particular as the convenient and effective energy filter for the quasiparticles.

In this paper, we consider one of the abovementioned structures, namely, the Lieb lattice. We focus our attention on the transmission of pseudospin-1 fermions in the quasi-periodic superlattices based on the Lieb lattice. The transmission spectra of quasiparticles are calculated and analyzed in dependence on the problem parameters. As far as we know, no attempt has been undertaken to investigate the problem of pseudospin-1 quasiparticles transport in the quasi-periodic structures.

2. METHOD OF CALCULATING OF THE TRANSMISSION SPECTRA

The Lieb lattice is schematically represented in Fig.1

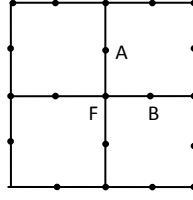


Figure 1. Schematic illustration of the Lieb lattice.

The elementary cell contains three atoms designated as A, B, F. There are three sublattices associated with these atoms. For small energies, the Schrödinger equation for the system considered can be deduced from a nearest neighbour tight-binding model Hamiltonian [8, 11, 15] and reads:

$$(-i\hat{S}\cdot\nabla + \Delta I + UI_0)\Psi = E\Psi, \quad (1)$$

where we accepted the units of measurement in which $\hbar = v_F = 1$, v_F the Fermi velocity (which is associated with the hopping (\hbar) and the lattice (a) constants as $v_F = \hbar a$), \hat{S} the pseudospin-1 operator with the components:

$$S_x = \begin{pmatrix} 0 & 1 & 0 \\ 1 & 0 & 0 \\ 0 & 0 & 0 \end{pmatrix}; \quad S_y = \begin{pmatrix} 0 & 0 & 0 \\ 0 & 0 & 1 \\ 0 & 1 & 0 \end{pmatrix}; \quad S_z = \begin{pmatrix} 0 & 0 & -i \\ 0 & 0 & 0 \\ i & 0 & 0 \end{pmatrix} \quad (2)$$

The second term on the left-hand side of formula (1) corresponds to the site-energy on the three sublattices, and

$$I = \begin{pmatrix} 1 & 0 & 0 \\ 0 & -1 & 0 \\ 0 & 0 & 1 \end{pmatrix} \quad (3)$$

There are three branches of the dispersion relation for the structure considered. For the massless particles ($\Delta = 0$), they are represented by the two cones contiguous in a Dirac point and giving a linear dependence of the energy on the quasi-momentum; the third branch forms a nondispersive planar band, also passing through the Dirac point. In the case of massive particles there is an energy gap between the cones of the value of 2Δ , and the mass of particles in the adopted units is equal to Δ .

The third term in the left side of the Schrödinger equation (1) represents the external potential $U(I_0)$ unit matrix).

Because of the translational invariance of equation (1) with respect to the Oy axis the wave function can be written as $\Psi(x, y) = \psi(x)e^{iky}$ and the components of the eigenfunction depending on x are of the form:

$$\begin{pmatrix} \psi_A(x) \\ \psi_F(x) \\ \psi_B(x) \end{pmatrix}_j = a_j \begin{pmatrix} \alpha_{xj} \\ 1 \\ \alpha_{yj} \end{pmatrix} e^{ik_{xj}x} + b_j \begin{pmatrix} -\alpha_{xj} \\ 1 \\ \alpha_{yj} \end{pmatrix} e^{-ik_{xj}x} \quad (4)$$

where the index j enumerates the potential barriers; expressions for α are given below.

Using the known boundary conditions to the wave functions which describe the fermionic states in the Lieb lattice [7], one can obtain the following expression for the transfer matrix that carries the solution from the point x to the point $x + \delta x$:

$$M_j = \begin{pmatrix} \cos(k_{xj}\delta x) & i\alpha_{xj} \sin(k_{xj}\delta x) \\ i\alpha_{xj}^{-1} \sin(k_{xj}\delta x) & \cos(k_{xj}\delta x) \end{pmatrix} \quad (5)$$

The transmission coefficient for the quasiparticles travelling through the superlattice is equal to

$$T = \left| \frac{2\alpha_{xw}}{\alpha_{xw}^2 R_{21} - \alpha_{xw}(R_{11} + R_{22}) + R_{12}} \right|^2, \quad (6)$$

where the matrix R is expressed with the help of the product of matrices M_j : $R = \prod_{j=1}^N M_j$, N - the number of barriers in the SL; for massless particles we have $\alpha_{xw} = \cos \varphi$; $\alpha_{yw} = \sin \varphi$; $\alpha_{xb} = \cos \theta$; $\alpha_{yb} = \sin \theta$; $\varphi = \arctan \frac{k_y}{k}$; $\theta = \arctan \frac{k_y}{q}$; $k = \sqrt{E^2 - k_y^2}$; $q = \sqrt{(E - U)^2 - k_y^2}$; in the case of massive particles expressions for the quantities related to α are given further (after the formula (9)) and are designated as α' . We consider the superlattice which contains the finite number of periods. Energy intervals in which the value of T is close to one form the allowed bands, values of $T \ll 1$ correspond to the forbidden bands.

3. RESULTS AND DISCUSSION

Since the double-barrier structure (DBS) is a basic element of a superlattice (element that comprises the quantum well), it is natural that the characteristics which describe the process of tunneling through the quasi-periodic SL have a certain connection with the characteristics of the transmission through the double-barrier structure. Therefore, for better understanding of the transmission through the quasi-periodic SL it is appropriate first to consider briefly some features of passing of particles through the DBS. For the double-barrier structure based on the Lieb lattice one can deduce an explicit expression for the transmission rates T depending on the energy of the incident on DBS massless quasiparticles E :

$$T(\text{DBS}) = \left\{ 1 + \left(\frac{\cos^2(\varphi) - \cos^2(\theta)}{\cos \varphi \cos \theta} \right)^2 \left[\cos(kw) \cos(qb) - \frac{1}{2} \left(\frac{\cos^2(\varphi) - \cos^2(\theta)}{\cos \varphi \cos \theta} \right) \sin(kw) \sin(qb) \right]^2 \sin^2(qb) \right\}^{-1} \quad (7)$$

Note that in the case of normal incidence of the quasiparticles on the structure its quantum transparency is perfect, i.e. $T = 1$, which corresponds to a phenomenon known as the Klein tunneling, and which is observed in particular in graphene [2].

Figs. 2 (a), (b) represent the transmission spectra for massless fermions through the double-barrier structure based on the Lieb lattice; parameters of the DBS are: $b = w = 1$, $U = 3$ for (a) and $U = 8$ for (b), the angle of incidence of particles on the structure $\varphi = \pi / 3$, $\Delta = 0$.

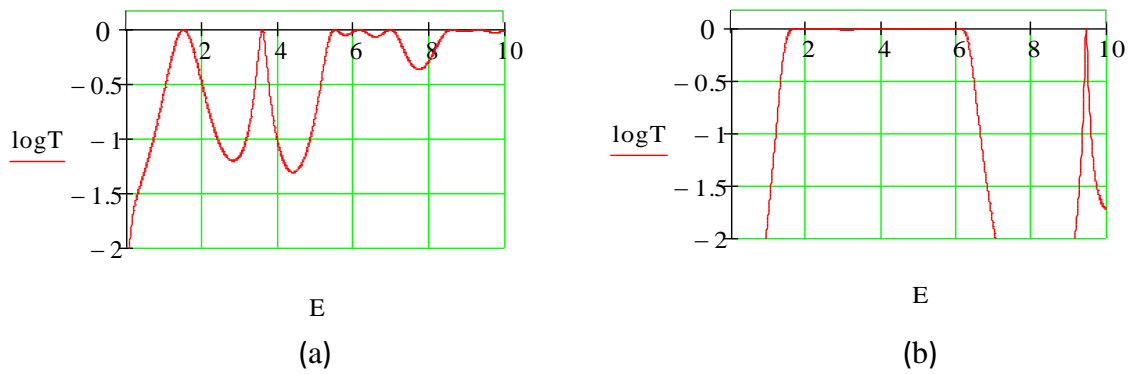


Figure 2. Dependence of the transmission rates T on energy E for the double barrier structure; the barrier height U is equal to 3 and 8 for (a) and (b) respectively; other parameters are as follows: $b = w = 1$, the angle of incidence of particles on the structure $\varphi = \pi / 3$, $\Delta = 0$.

It is seen in the spectra that the energy areas for which the transmission coefficient T is close to one alternate with the ranges for which the values of T is much less than unity - this suggests that this DBS based on the Lieb lattice is a resonant tunneling structure (DBRTS).

For the energy equal to half the height of the potential barrier, there is a phenomenon which was called in the literature as the superKleintunneling (all-angle tunneling) [6-18]: for this energy, the transparency of the systems with the pseudospin-1 quasiparticles is equal to unity ($T = 1$) for any angle of incidence of the particles on the given structure. (Naturally, this result is true not only for equal values of quantities of band w).

Note that in the vicinity of the point $E = U/2$, the plateau of energies is formed for which the transmission coefficient is close to unity. This plateau can be of a different width depending on the parameters of the problem, in particular, on the height of the potential barrier. Fig. 2 (b) shows the transmission spectrum for DBRTS with the same parameters as in Fig. 2 (a), but with the value $U = 8$, the plateau in this case being much wider than in Fig. 2 (a). This plateau is robust with respect to changes in the parameters of the structure; for its separation into individual peaks (resonances) fairly large values of the "barrier area" are required (the quantity which is the product of the barrier width by its height $b \cdot U$) - either by b , or due to U . The existence of this plateau with high transmission coefficient values is a fact proving that the structures with the pseudospin-1 quasiparticles are characterized by higher quantum transparency than the systems with pseudospin-1/2 particles [7].

With an increase in the lattice periods number, the transformation of the special band associated with the $U/2$ point differs from the changes of other bands, which are typical: their width increases and the structure of resonance peaks is formed inside each band, the number of peaks increasing with the number of the superlattice periods. The special band

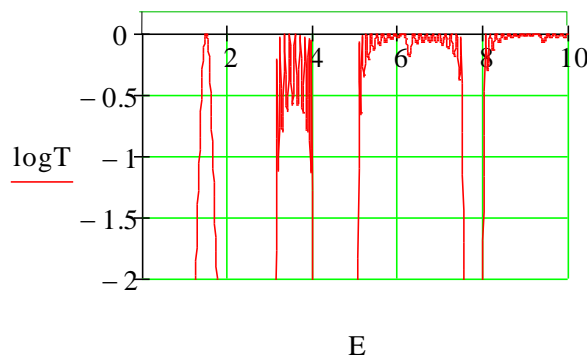


Figure 3. Log T vs E dependence for the SL containing 10 periods; other parameters are as follows: $U = 3$, $b = w = 1$, $\varphi = \pi / 3$, $\Delta = 0$.

remains narrow and does not have the structure of resonant peaks, see Fig. 3; the parameters are as follows: $U = 3, b = w = 1, \varphi = \pi / 3, \Delta = 0$, the number of periods is equal to 10.

It is known that for the structures made on the base of graphene and the graphene-like materials, resonant states may originate not only from the quantum wells but also from the barriers. With an increase in the barrier thickness the energy plateau in the transmission spectra remains but becomes narrower; a number of new resonances of the barrier nature appears, as shown in Fig. 4; the parameters of the SL are as follows: $b = 10, w = 1, U = 8, \varphi = \pi / 3, \Delta = 0$.

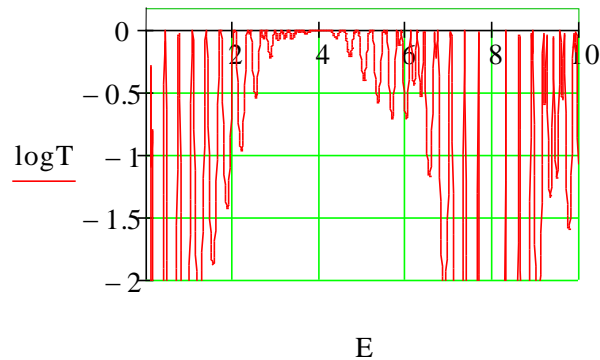


Figure 4. Log T vs E dependence for the SL with the thick barriers; values of the parameters are as follows: $b = 10, w = 1, U = 8, \varphi = \pi / 3, \Delta = 0$.

Now consider the transmission of pseudospin-1 fermions through the quasi-periodic superlattice based on the Lieb lattice.

For our analysis, we have taken the most studied, classical Fibonacci superlattice, the elements of which are arranged along the SL chain according to the Fibonacci inflation rule. The lattice is constructed of two separate elements A and B according to the rule: $S_n = S_{n-1} + S_{n-2}$, where n is the number of sequence (for example, for the fourth Fibonacci generation $S_4 = ABAAB$).

As elements A and B, we take the potential barriers of the heights U_A and U_B respectively and of the same width b . Barriers are considered to be rectangular, they are arranged along the superlattice axis Ox and their width is substantially greater than the distance between the nearest sites of the Lieb lattice. The widths of the quantum wells disposed between the barriers are considered to be the same and equal to w .

Fig. 5 illustrates the potential profile of the superlattice that relates to the second Fibonacci generation. Letters U_A and U_B designate the barrier regions (with the width b) of the superlattice and the quantum wells (with the width w) are located between the barriers.

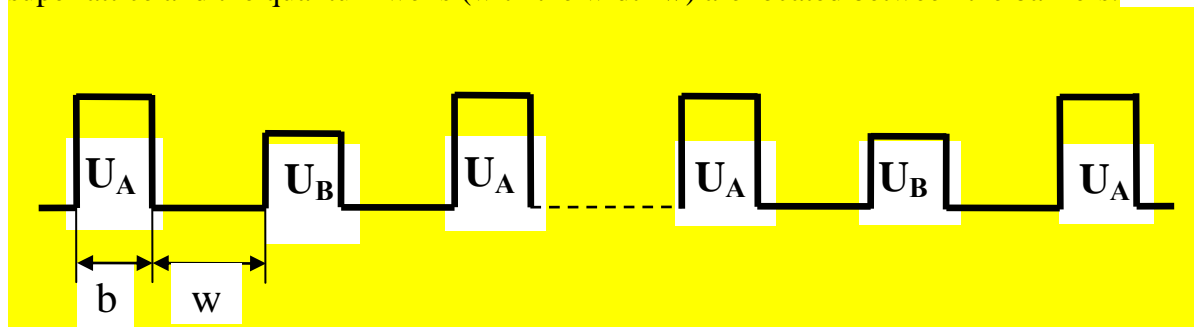


Figure 5. The potential profile of the superlattice that relates to the second Fibonacci generation. Letters U_A and U_B designate the barrier regions (with the width b) of the superlattice and the quantum wells (with the width w) are located between the barriers.

Terms of passage of the quasi-electron wave through the SL built for the n -th Fibonacci generation are determined by the period of this generation.

Fig. 6 shows a typical trace map for the initial iterations of the Fibonacci superlattice built of the Lieb lattice, values of the parameters are as follows: $b=w=1, U_A \equiv U=3, U_B=0$, the mass terms in both SL elements are equal to zero: $\Delta_A = \Delta_B = 0; \varphi = \pi/3$. Solid lines correspond to the allowed bands. In general, the number of bands in a fixed energy range of the spectrum depends on the generation level and the parameters of the superlattice. With the growth of the iteration level, splitting of the allowed bands is observed, and their total width decreases with transition to each higher generation (total width of gaps increases).

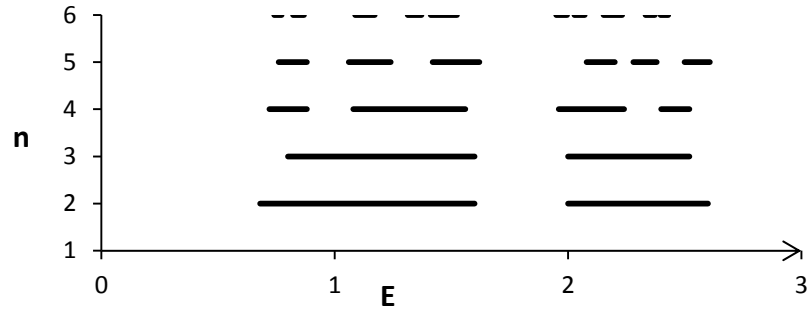


Figure 6. Trace map for the SL with massless quasi-particles; values of the parameters are as follows: $b=w=1, \Delta_A = \Delta_B = 0; \varphi = \pi/3, U_A = 3, U_B = 0$.

We see that an effective quasi-periodical modulation is observed. It is easy to check that wide gaps in the spectra originate from the strictly periodic SL, while the narrow gaps are due to the quasi-periodical factor. (Naturally, this is true not only for equal values of quantities of b and w).

The spectra of higher generations are strongly fragmented, and the fragmentation degree increases significantly with the increase in geometrical SL parameters b, w . The fragmentation of the allowed bands in all generations starting from the third one happens in accordance with the property of self-similarity.

The trace map depicted in Fig. 6 reveals properties that are in some aspects essentially different from the analogous trace maps of the graphene structures [25, 26, 29, 31, 33, 35]:

1. Particular attention is attracted to the point of energy $E = U/2$. For all Fibonacci generations, the super Klein tunneling is observed for this energy. This differs drastically from the case of graphene, where the superlattice Dirac gap appears at the point $U/2$ in a wide range of the parameter values [3, 25, 33, 36]. For example, it is shown in ref. [25] that the Dirac gap appears at the point $E_D = bU/(b+w)$ which is equal to $U/2$ in the case where the widths of the barrier b and the quantum well w are equal (transmission spectra through the graphene Fibonacci sequences were calculated in [25] under the condition of the oblique incidence of electrons on the superlattice).

2. The value of T is close to one in the vicinity of $E = U/2$, and this special energy zone is very robust (stable) with respect to the influence of the quasi-periodic factor. Thus, splitting of this zone occurs not in the third but only in the fourth generation. It should be noted that in the barrier region, i.e. within the energy range $[0, U]$, the number of the allowed bands in each following sequence is subjected to the Fibonacci rule: $Z_n = Z_{n-1} + Z_{n-2}$, namely, the number of zones for the 3rd, 4th, 5th, 6th ..., generations are equal to 2, 4, 6, 10... respectively.

3. For the stronger quasi-periodic factor, i.e. for greater difference between the values of U_A and U_B , we observe the following changes in the trace-map: 1) more significant reduction of the allowed bands; 2) a shift of the bands toward higher energies. It differs greatly from the graphene-based SL, in which the trace map composition (i.e. mutual arrangement of bands) does not change with amplification of the quasi-periodic factor (there is no shift of the bands, see, e.g. [33, 35]).

The performed calculations show that the effective quasi-periodic modulation of the transmission can also be carried out in the SL based on the Lieb lattice with the massive particles. Moreover, in this case the quasi-periodic modulation is found both for the oblique and for the normal incidence of the quasiparticles. Same as for the massless particles, the quasi-periodic modulation may be provided via the alternation of the of the potential barriersheights U_A and U_B . Fig.7represents the trace map for the primary sequences of the Fibonacci superlattices; the parameters are as follows: $b=w=1, U_A \equiv U=0.8; U_B=0; \Delta = 0.4$, the particles fall normally to the lattice.

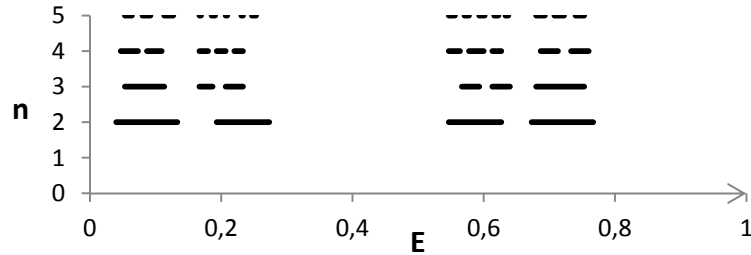


Figure 7.Trace map for the SL with the massive quasi-particles for a special case: $U=0.8, U_B=0, \Delta=U/2$; values of other parameters are as follows: $b=w = 1, \varphi = 0$.

In contrast to the case of $\Delta = 0$, the splitting of the allowed bands located near the point $E= U/2$ occurs already in the third generation.

The bandsplitting happens in accordance with the inflation Fibonacci rule: for the parameters taken, the numbers of bands for the 2nd, 3rd, 4th, 5th, generations are equal to 4, 6, 10, 16,... respectively. Note that for the massive particles the number of bands in a fixed energy range may depend on the value of the parameter Δ .

There is a wide gap in the vicinity of the point $U/2$. It is much wider than other gaps. The crucial feature here is that the gap is formed at an arbitrary angle of incidence. This differs drastically from the case of massless particles, where the transparency maximum is observed at the point $U/2$, as mentioned above. Because of these opposite cases we can speak here not only of the super Klein tunneling (the case of $\Delta =0$), but also of the super reflection, meaning that it occurs at an arbitrary angle of incidence.

As previously indicated, it is clear that the spectral characteristics of superlattices are closely related to the characteristics of the double-barrier resonant tunneling structures. Using the Bloch theorem, we can write the following equation for DBRTS

$$\cos(k_B \lambda) = \frac{1}{2} \text{Tr}(M_A M_B M_A) \quad (8)$$

Substituting the explicit form of the matrices M_B, M_A in expression (8), we obtain the transcendental equation

$$\cos(k_b \lambda) = \cos(kw) \cos(2bq) - \left(\frac{\alpha'_{xb}}{\alpha'_{xw}} + \frac{\alpha'_{xw}}{\alpha'_{xb}} \right) \sin(qb) \sin(kw) \cos(qb) \quad (9)$$

where k_b is the Bloch quasi-momentum, λ the SL period,

$$\alpha'_w = \sqrt{\frac{E^2 - \Delta^2 - k_y^2}{E - \Delta}}; \quad \alpha'_b = \sqrt{\frac{(E - U)^2 - \Delta^2 - k_y^2}{E - U - \Delta}}$$

The analysis of this expression shows that, unlike for the massless fermions, in a wide range of the parameters of the problem considered, we observe not the allowed but the forbidden

band in the vicinity of the energy $E=U/2$. This conclusion is also valid for the tracemaps of the quasi-periodic SL based on the Lieb lattice.

In addition, we note that for the massive quasi-particles the following changes in the spectra are observed. When the value of Δ is small, the mass does not exert a strong effect on the transmission spectra. Thus, e.g., we see in Fig. 8 for the spectra for the third Fibonacci iteration level,

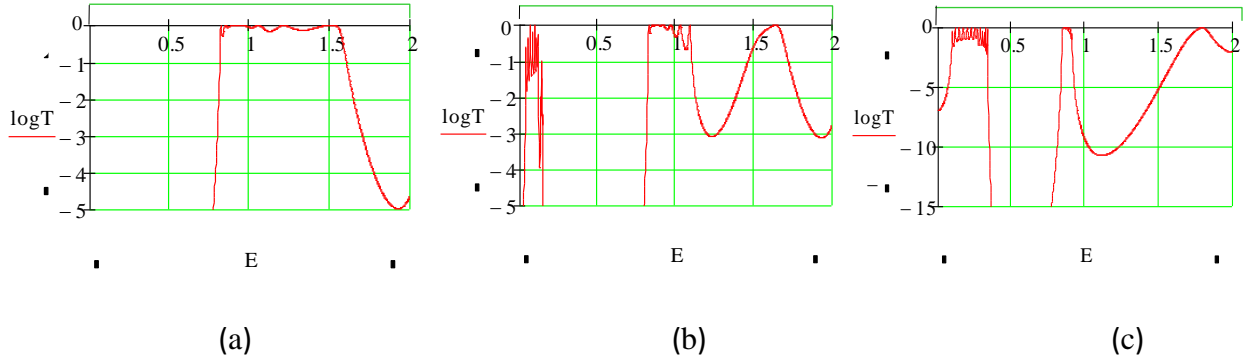


Figure 8. Log T vs E dependence for the third Fibonacci iteration with different values of $\Delta = 0, \Delta = 0.2, \Delta = 0.4$ for figures (a), (b), (c) respectively; $b=w=1, U=2, \varphi = \pi/3$.

that the allowed band near the point $U/2$ (which is similar to the special band in the case of the massless particles) is narrowed, and a mass term leads to the separation of the resonance corresponding to the point $U/2$ from the band, and at the same time it causes the shift of the resonant peak from the point $U/2$ towards higher energies (Fig. 8 (b) for $\Delta = 0.2$). Nevertheless, for larger values of Δ , for example for $\Delta = 0.4$, the presence of a wide gap near the point $U/2$ is already observed (Fig. 8 (c)).

Fig. 9 represents the tracemap for more general case comparing with the special case of Fig. 7 (where $\Delta = U/2$), the parameters are as follows:

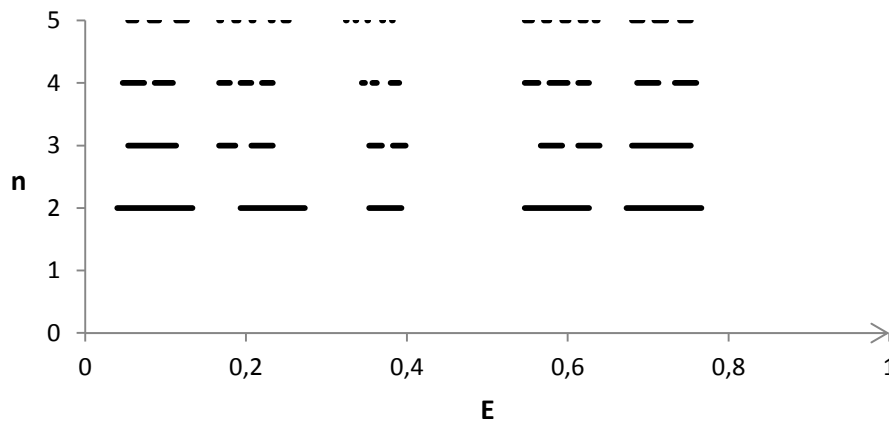


Figure 9. The trace map for the SL with massive particles in general. The parameter values are as follows: $b=w=1, U=0.8, \Delta=0.45, \varphi = 0$.

$U=0.8, \Delta=0.45, b=w=1$. Comparing the last two trace maps, we note that there is a significant difference between them. It is related to the behavior of particles at energies close to the value of $U/2$. We observe the additional bands in every generation; they adhere to the Fibonacci inflation rule. Total band number also agrees with the Fibonacci rule: we have 5, 8, 13, 21, ... bands for

the 2nd, 3rd, 4th, 5th, ...sequence. To clarify the difference illustrated by Fig.7 and Fig.9 consider the spectra for the DBRTS shown in Fig.10 (a) and 10 (b) with the parameter values: $b=w=1$, $U=1, \varphi = 0$, $\Delta = 0.49 U$ and $\Delta = 0.4999 U$ for figures (a), (b) respectively.

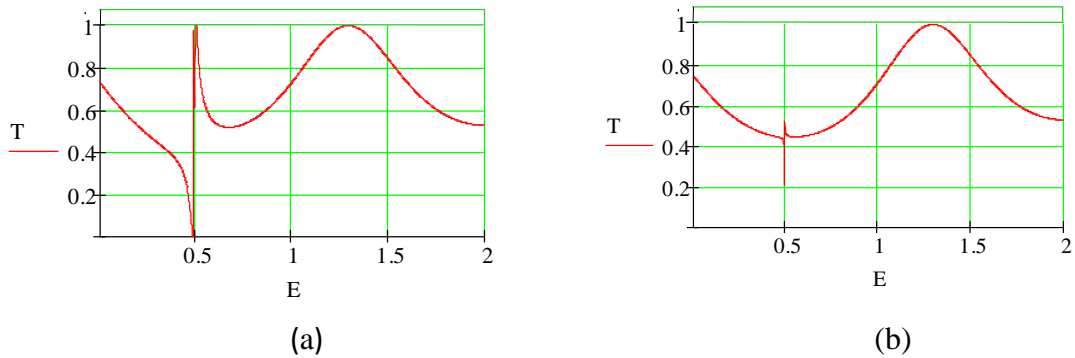


Figure 10. T vs E dependence for the DBRTS, $\Delta = 0.49 U$ and $\Delta = 0.4999 U$ for figures (a), (b) respectively; $b=w=1$, $U=1, \varphi = 0$.

The behavior of the curves in Fig. 10 (a) and Fig. 10 (b) can be explained by the following. In a close vicinity of the point $E = U/2$, when the equation $\Delta=U/2$ holds, there are two tendencies: on the one hand, the effect of quasi-momentum minimization leads to a minimum T value (similar to the situation in [37]), on the other hand, maximal T can also be produced in a given structure at the point $U/2$. As a result, sharp maximum and minimum of the curves are observed in the spectra shown in Fig. 10 (a) and Fig. 10 (b). In the multibarrier structures, an additional band of the resonance states is formed at this point. When the equation $E = U/2 = \Delta$ is precise there is no additional band, since the minima and maxima compensate each other.

Note that at the energy point $E = U/2$ when the value Δ is close but not equal to $U/2$, anti-resonant states are observed (see Fig.10 (a)).

It is well known that graphene and the graphene-based structures may exhibit unusual properties for a special choice of the parameter values. The same is also true for the structures based on the Lieb lattice. These properties, as well as the phenomenon of the super Klein tunneling, relate to the energy equal to half the height of the potential barrier. Namely, when the mass term Δ is equal to $U/2$, the transmission spectra of the SL based on the Lieb lattice (where the particles have pseudospin-1) are identical with the spectra of the SL based on the gapped graphene (where the quasi-particles have pseudospin equal to $1/2$).

An example of such a spectrum for the third Fibonacci generation is shown in Fig.11, the parameters are as follows: $d=w=2$, $U=0.8$, $\Delta_A=0.4$, $\Delta_B=0$.

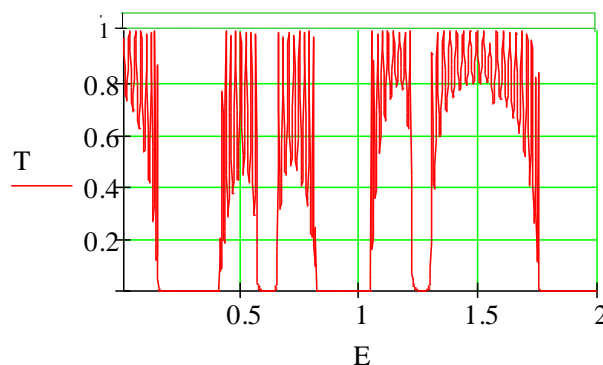


Figure 11. T vs E dependence for the third Fibonacci generation for the special set of the parameters: $d=w=2$, $U=0.8$, $\Delta_A=0.4$, $\Delta_B=0$.

Conductivity of the structures discussed in this paper is commonly expressed in terms of the transmission rates. In the case of low temperatures it is calculated with the help of the Landauer-Buttiker formula:

$$G = \int_0^{\pi/2} T(E, k_y) \cos \theta d\theta, \quad (10)$$

where G is the dimensionless conductivity [38].

Calculations show that the transmission rates in this structure weakly depend on the incidence angle of the quasiparticles (in a wide range of incidence angles and in agreement with the results of e.g. [7, 12, 15] where T value for a single barrier is calculated). Therefore, using the formula (10) – which is the averaged conductivity over incidence angles – this quantity as the function of energy has the same qualitative course as the transmission coefficient dependence on energy. However, there is a fact that significantly differentiates the dependencies $G(E)$ and $T(E)$. Fig. 12 shows energy dependence of conductivity for the 3rd Fibonacci generation for the SL considered in this paper.

For this figure, we chose the parameter values for which transmission rates values in the vicinity of the point $E = U/2$ are not high: $d=w=1$, $U=0.6$, $\Delta_A=\Delta_B=0.3$ (see the comment to Figs. 7, 9). Nevertheless, conductivity as the function of energy reveals high values in the indicated vicinity, see region “c” in Fig. 12. This results from high T values for incidence angles other than zero. At the same time, since according with the formula (10) normally incident particles give the main contribution to the conductivity, the energy range near the point $E = U/2$, where $G(E)$ has sufficiently high value, is very narrow (see region “c” in Fig.12), and conductivity itself does not reach its maximum value (compare with a number of other energy ranges “a”, “b”, “d”, “e”, “f” in the same figure).

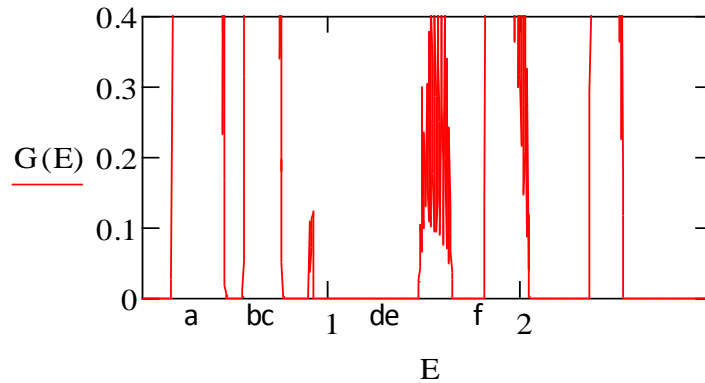


Figure 12. The dependence of the dimensionless conductivity on energy of the SL for the third Fibonacci generation; the parameter values: $d=w=1$, $U=0.6$, $\Delta_A=\Delta_B=0.3$.

4. SUMMARY

This paper considers the ballistic transport of the pseudospin-1 fermions in the structures based on the Lieb lattice, mainly in the quasi-periodic Fibonacci superlattices. The trace maps are calculated for the initial Fibonacci generations. It is concluded that the effective quasi-periodic modulation may be achieved for the massless as well as for the massive quasiparticles. For the massless particles, the phenomenon of super Kleintunneling is observed in all Fibonacci generations. For the massive particles, in all Fibonacci generations an energy gap is

formed in the vicinity of the point $E=U/2$ (U is the barrier height) in a wide range of the parameter values. Transmission spectra of the quasi-periodic superlattices obey the rules of splitting inherent to the Fibonacci structures. Some features of the transmission spectra for the quasi-periodic superlattices based on the Lieb lattice and on the other hand for the graphene-based structures were discussed, and it is noted that for a special choice of parameter values of the spectra of quasiparticles with the pseudospin equal to one half, and the pseudospin equal to unity, are completely the same.

It's a pleasure for the authors to express our gratitude to O.A.Sokolenko for the technical assistance.

References

- [1] A.K. Geim, K. S. Novoselov, *Nature Mater.* 2006, 6, 183.
- [2] A. H. Castro Neto, F. Guinea, N. M. R. Peres, K. S. Novoselov, A. K. Geim, *Rev. Mod. Phys.* 2009, 81, 109.
- [3] Li-Gang Wang, Shi-Yao-Zhu, *Phys. Rev. B* 2010, 81, 205444.
- [4] C.-H. Park, L. Yang, Y.-W. Cohen, S.G. Louie, *Nat. Phys.* 2008, 4, 213.
- [5] S. K. Choi, C.-H. Park, S. G. Louie, *Phys. Rev. Lett.* 2014, 113, 026802.
- [6] Balázs Dóra, Jani Kailasvuori, R. Moessner, *Phys. Rev. B* 2011, 84, 195422.
- [7] Daniel F. Urban, Dario Bercioux, Michael Wimmer, Wolfgang Hausler, *Phys. Rev. B* 2011, 84, 115136.
- [8] D. Leykam, Omri Bahat-Treidel, A. S. Desyatnikov, *Phys. Rev. A* 2012, 86, 031805(R).
- [9] Yafang Xu, Guojun Jin, *Physics Letters A* 2014, 378, 3554.
- [10] Hong-Ya Xu, Ying-Cheng-Lai, *Phys. Rev. B* 2016, 94, 165405.
- [11] A. Fang, Z.Q. Zhng, Steven G. Louie, C. T. Chan, *Phys. Rev. B* 2016, 93, 035422.
- [12] Rhu Zhu, Pak Ming Hui, *Physics Letters A* 2017, 381, 1921.
- [13] D. Bercioux, D. F. Urban, H. Grabert, W. Häusler, *Phys. Rev. A* 2009, 80, 063603.
- [14] H.-M. Guo, M. Franz, *Phys. Rev. B* 2009, 80, 113102.
- [15] R. Shen, L. B. Shao, Baigeng Wang, D. Y. Xing, *Phys. Rev. B* 2010, 81, 041410.
- [16] S. Mukherjee, A. Spracklen, D. Choudhury, N. Goldman, P. Öhberg, E. Andersson, R.R. Thomson, *Phys. Rev. Lett.* 2015, 114, 245504.
- [17] Zeren Lin, Zhirong Liu, *Journal of Chemical Physics* 2015, 143, 214109.
- [18] E. Illes, E. J. Nicol, *Phys. Rev. B* 2017, 95, 235432.
- [19] R. Tsu, *Superlattice to Nanoelectronics*, Elsevier, Oxford, 2005.
- [20] H. Cheng, R. Savit, R. Merlin, *Phys. Rev. B* 1988, 37, 375.

- [21] E.Macia, *Rep. Phys.*2012, 75, 036502.
- [22] J.M. Luck, *Phys. Rev. B*1989, 39, 5834.
- [23] M.Kolar, M.K.Ali, F. Nori, *Phys. Rev. B*1991, 43, 1034.
- [24] N. Liu, *Phys. Rev. B*1997, 55, 3543.
- [25] P. Zhao, X. Chen, *Appl. Phys.Lett.* 2011, 99, 182108.
- [26] Lu Wei- Tao, Wang Shun-Jin, Wang Jong-Long, Jiang Hua, Li Wen. *Physics Letters.A*2013, 377, 1368.
- [27] XuYafang, ZouJianfei, Jin Guojun. *J. Phys.Condens. Matter.*2013, 25, 245301.
- [28] S. H. R.Sena, J. M. Pereira Jr, G. A.Farias, M. S.Vasconcelos, E. L.Albuquerque, *J. Phys.: Condens. Matter.*2010, 22,465305.
- [29] S. Mukhopadhyay, R. Biswas, C.Sinha.*Physica Status Solidi(b)* 2010, 247, 342.
- [30] Haiyan Liu, Hongmei Zhang, De Lie, *Physics LettersA*2015, 379, 192.
- [31] Changan Li, Hemeng Cheng, Ruofan Chen, Tianxing Ma, Li-Gang Wang, Yun Song, and Hai-Qing Lin. arXiv:1308.3965v2 [cond-mat.str-el] 14 Oct2013.
- [32] Rogelio Rodrigues-Gonzalez, Isaac Rodriguez-Vargas, Dan Sidney Diaz-Guerrero, Luis Manuel Gaggero-Sager, *European Physical JournalB*2016, 89:17.
- [33] A. N. Korol, V.N. Isai, *Physics of the solid state.*2013, 55,2596.
- [34] A. N. Korol, *Low Temperature Physics.*2014, 40, 324.
- [35] A.M. Korol, S.I. Litvynchuk, *Physica Status Solidi(b)*,2017, 254, 1600381.
- [36] L.-G. Wang, X. Chen, *Appl. Phys.* 2011, 109, 033710.
- [37] M.Barbier, F.M.Peeters, P. Vasilopoulos, J. Milton Pereira, *Phys. Rev. B*2008, 77, 115446.
- [38] NeetuAgrawal (Garg), Sameer Grover, SankalpaGhosh, Manish Sharma, *J. Phys.Cond. Matt.* 2012, 24, 175003.
- [39] Y. Betancur-Ocampo, G. Cordourier-Maruri, V.Gupta, R. de Coss, *Phys. Rev.B*,2017, 96, 024304.
- [40] H.Garcia-Cervantes, J. Madrigal-Melchor, J. C. Martinez-Orozco, I. Rodriguez-Vargas, *Physica B*, 2017, 478, 99.
- [41] T.Q. Araujo, Jonas R.F. Lima, *Physics Letters A*, 2017, 381, 3228.
- [42] Mingjing Wang, Hongmei Zhang, De Liu, *Physica E*, 2018, 98, 140.
- [43] J.D. Malcolm, E.J. Nicol, *Phys. Rev. B*, 2015, 92, 035118.
- [44] S.Peotta, P.Torma, *Nat. Commun.* 2015, 6, 8944.
- [45] A.Julku, S.Peotta, T.I. Vanhala, D.H. Kim, P. Torma, *Phys.Rev.Lett*, 2016, 117, 045303.

[46] P.E.Allain, J.N.Fuchs, *European Physical Journal B*, 2011, 83, 301.